Geosci. Model Dev. Discuss., 5, 2789–2809, 2012
www.geosci-model-dev-discuss.net/5/2789/2012/
doi:10.5194/gmdd-5-2789-2012

Geoscientific Model Development Discussions

A methodology for estimating seasonal cycles of atmospheric CO_2 resulting from terrestrial net ecosystem exchange (NEE) fluxes using the Transcom T3L2 pulse-response functions

C. D. Nevison[1], D. F. Baker[2], and K. R. Gurney[3]

[1]Institute for Arctic and Alpine Research, University of Colorado, Boulder, Colorado, USA
[2]Cooperative Institute for Research in the Atmosphere, Colorado State University, Fort Collins, Colorado, USA
[3]School of Life Sciences, Arizona State University, Tempe, AZ, USA

Received: 9 August 2012 – Accepted: 1 September 2012 – Published: 12 September 2012

Correspondence to: C. D. Nevison (cynthia.nevison@colorado.edu)

Published by Copernicus Publications on behalf of the European Geosciences Union.

Abstract

We present a method for translating modeled terrestrial net ecosystem exchange (NEE) fluxes of carbon into the corresponding seasonal cycles in atmospheric CO_2. The method is based on the pulse-response functions from the Transcom 3 Level 2 (T3L2) atmospheric tracer transport model (ATM) intercomparison. The new pulse-response method is considerably faster than a full forward ATM simulation, allowing CO_2 seasonal cycles to be computed in seconds, rather than the days or weeks required for a forward simulation. Further, the results provide an estimate of the range of transport uncertainty across 13 different ATMs associated with the translation of surface NEE fluxes into an atmospheric signal. We evaluate the method against the results of archived forward ATM simulations from T3L2. The latter are also used to estimate the uncertainties associated with oceanic and fossil fuel influences. We present a regional breakdown at selected monitoring sites of the contribution to the atmospheric CO_2 cycle from the 11 different T3L2 land regions. A test case of the pulse-response code, forced by NEE fluxes from the Community Land Model, suggests that for many terrestrial models, discrepancies between model results and observed atmospheric CO_2 cycles will be large enough to clearly transcend ATM uncertainties.

1 Introduction

Net uptake of CO_2 on land and in the ocean has absorbed on average more than half of the total anthropogenic carbon input from fossil fuel combustion, cement manufacture and deforestation over the last 50 yr (Forster et al., 2007). Future increases in atmospheric CO_2 therefore depend not only on fossil fuel consumption but also on future CO_2 uptake by land and ocean sinks. However, predictions of these future sinks by ocean biogeochemistry and terrestrial ecosystem models vary dramatically (Friedlingstein et al., 2006). To improve confidence in projected atmospheric CO_2 levels, it is

GMDD
5, 2789–2809, 2012

critical that the land and ocean sinks be quantified as accurately as possible using mechanistic models that have been rigorously tested against present-day metrics.

The mean seasonal cycle in atmospheric CO_2 is a logical present-day metric since the changes in land or ocean biogeochemistry expected due to anthropogenic forcing over the next century are generally small compared to changes that occur naturally over a seasonal cycle. Furthermore, the seasonal cycles in atmospheric CO_2 are well documented and reflect the integrated effects of surface carbon fluxes over large regions. The seasonal cycle in atmospheric CO_2 occurs mainly due to a seasonal imbalance between terrestrial net primary production and heterotrophic respiration known as net ecosystem exchange (NEE) (Fung et al., 1987; Keeling et al., 1996). In contrast, fossil fuel emissions are thought to have only a small seasonality (Rotty, 1987; Blasing et al., 2005) and air-sea CO_2 fluxes are strongly damped on seasonal time scales by ocean carbonate chemistry (Takahashi et al., 2002).

Use of the atmospheric CO_2 seasonal cycle to evaluate surface carbon fluxes has the drawback that atmospheric tracer transport models (ATMs) are needed to translate the surface fluxes into an atmospheric signal. Transport differences among ATMs unavoidably create uncertainty, making it difficult to distinguish whether discrepancies between modeled and observed CO_2 cycles are due to problems with the surface fluxes themselves or with atmospheric transport (Gurney et al., 2002; Baker et al. 2006; Stephens et al., 2007). Furthermore, ATM simulations driven by multiple years of surface fluxes are time consuming to set up and run. Here, we present a new methodology that allows the atmospheric seasonal cycle in CO_2 resulting from terrestrial NEE to be quickly and efficiently estimated, while providing an estimate of the range of uncertainty in the signal predicted by 13 different ATMs.

2 Methodology

Our method is based on the archived "pulse-response" functions from the Transcom 3 Level 2 experiment (T3L2) (Gurney et al., 2004). T3L2 was designed to examine the

GMDD
5, 2789–2809, 2012

influence of ATM uncertainty on atmospheric CO_2 inversions, with emphasis on the mean seasonal cycle. As part of T3L2, each of 13 participating ATMs conducted forward simulations in which a pre-specified flux pattern, normalized to 1 Pg C yr^{-1}, was released from each of 22 regions (11 land, 11 ocean) for each of 12 "emission months," i.e. January–December. For the 11 land regions, the pre-specified spatial flux distributions were set to the annual mean Net Primary Productivity (NPP) patterns of the CASA Neutral Biosphere Model (Randerson et al., 1997). The simulations were run for 36 "measurement months," in which the pulses were turned on for the first month and shut off for the remaining 35 months, during which time the initial pulse became increasingly well mixed throughout the atmosphere. For each ATM, region, emission month and measurement month, the model atmospheric fields were sampled at each of 253 latitude/longitude/height coordinates corresponding to the locations of atmospheric monitoring sites. The resulting "pulse-response" functions, in units of ppm $(Pg\,C\,yr^{-1})^{-1}$, are footprints that represent the atmospheric signal corresponding to a unit surface pulse of CO_2.

We used the pulse-response functions to construct a matrix **H** (Fig. 1, Table 1). **H** is similar to the matrix used in Bayesian atmospheric inversions (Baker, 1999, 2001; Baker et al., 2006). Here we perform a simple matrix multiplication (Eq. 1) that estimates the atmospheric CO_2 time series resulting from a set of Net Ecosystem Exchange (NEE) fluxes:

$$\mathbf{H}\boldsymbol{f} = \boldsymbol{c}, \tag{1}$$

where $\boldsymbol{f}$ is a vector of monthly mean NEE fluxes in Pg C yr^{-1}, aggregated over a given land region and $\mathbf{c}$ is the corresponding atmospheric CO_2 time series in ppm. As described below, $\boldsymbol{f}$ is 3 yr longer than $\boldsymbol{c}$ to account for the influence of fluxes predating the measurement month by up to 3 yr. In cases where only a single year of fluxes is available, a vector $\boldsymbol{f}$ spanning N flux years can be constructed, in which the cyclostationary fluxes are repeated year to year. Applying Eq. (1) then yields a time series $\boldsymbol{c}$ of length

GMDD
5, 2789–2809, 2012

N – 3 years. N must be at least 4 to yield c of at least 1 yr, and ideally should be longer to permit easier detrending of $\boldsymbol{c}$ (we use N = 13 in this study).

The time series $\boldsymbol{c}$ can be analyzed using standard methods to derive the mean seasonal cycle in atmospheric CO_2. Here, the raw monthly mean time series $\boldsymbol{c}$ first was detrended with a 3rd order polynomial, then a monthly mean seasonal cycle was constructed by taking the average of the detrended data for all Januaries, Februaries, etc. In principle, $\boldsymbol{c}$ can also be analyzed for interannual variability (IAV), but it will only reflect IAV due to $\boldsymbol{f}$, rather than a combination of $\boldsymbol{f}$ and transport, since $\mathbf{H}$ uses an annually repeating cycle of meteorology. At each monitoring site, $\boldsymbol{c}$ is computed separately for each land flux region. The region-specific time series can either be aggregated over all regions to give the net atmospheric CO_2 signal or treated separately to estimate the contribution of each individual region to the CO_2 seasonal cycle.

To validate the results of our pulse response code, we used the forward "pre-subtracted tracer" simulations computed by each of the thirteen T3L2 ATMs (Gurney et al., 2004; Baker et al., 2006). These forward simulations were forced by fine-scale (0.5 × 0.5 deg) monthly mean net ecosystem exchange (NEE = heterotrophic respiration – NPP) fluxes from the CASA land biosphere model (Randerson et al., 1997). The simulations were run with the fluxes turned on for the first year and turned off for the last two years. The resulting ATM atmospheric CO_2 fields were sampled in each of the 36 months of the simulations at each of the 253 monitoring sites discussed above. The steady-state response, i.e. the mean seasonal cycle, was computed by summing all Januaries, Februaries, etc., for the three years. Conceptually, this calculation assumes that the ATM behaves linearly and that the steady-state response can be represented as the sum of the response to the fluxes from the present year, the past year, and two years previously, which correspond to the first, second, and third years of the simulations, respectively. Using the same methodology, we calculated the mean seasonal cycle due to fossil fuel and oceanic influences using the T3L2 "pre-subtracted tracer" forward simulations forced by oceanic net air-sea CO_2 fluxes and 1990 fossil fluxes (Andres et al., 1996; Takahashi et al., 1999; Gurney et al., 2004). These ocean and

GMDD
5, 2789–2809, 2012

fossil cycles were used to "correct" the observed atmospheric CO_2 cycle, as described below.

We used our pulse-response code, forced with the same $0.5^\circ \times 0.5^\circ$ CASA NEE fluxes used in the T3L2 forward simulations, to estimate the mean seasonal cycles at a subset of 60 of the T3L2 monitoring sites. As a validation exercise, these were compared to the mean seasonal cycle computed from the forward simulations of the NEE pre-subtracted tracer runs for each model. The comparison is presented for a single model (GCTM) at 16 selected stations (Fig. 2), while the comparisons for all 13 models, as well as the mean of all 13 models, at all 60 stations are summarized in a set of Taylor-type diagrams (Taylor, 2001) (Fig. 3).

Finally, as a test case of our model, we forced our pulse-response code with 13 yr of NEE fluxes corresponding to 1993–2005 from an online run of the Community Land Model (CLM4) with realistic transient forcing from increasing atmospheric CO_2 and nitrogen deposition (Bonan and Levis, 2010). We derived the corresponding mean seasonal cycle in atmospheric CO_2 as described above.

3 Results

The pulse-response code (PRC) forced with CASA NEE fluxes successfully captures the general shape and amplitude of the mean CO_2 seasonal cycle from the archived T3L2 forward simulations (FS) across a range of surface monitoring stations, spanning from the South Pole to Alert, Greenland (Fig. 2). The GCTM model is chosen to illustrate this validation exercise, but similar results are obtained for the other twelve T3L2 ATMs. As shown in the summary Taylor diagrams (Fig. 3), the PRC performs best in the Northern Hemisphere, where the correlation coefficient (polar axis) for PRC vs. FS at most stations is $R = 0.95$ or better, and the amplitude ratio (represented by the ratio of standard deviations: σ_{prc}/σ_{fs} on the radial axis) typically centers around 1. In the Southern Hemisphere, the PRC performance is generally weaker, although some models (e.g. TM2, CSU) still reproduce the FS seasonal cycles well.

GMDD
5, 2789–2809, 2012

The pulse-response code is also useful for estimating which land regions contribute to the total NEE-driven seasonal cycle in atmospheric CO_2 at different monitoring sites (Fig. 4). Boreal Eurasia and Boreal North America both make important contributions to the seasonal cycle at Barrow, Alaska, with lesser contributions from Europe and Temperate North America. At Park Falls, Wisconsin, the contribution from Temperate North America dominates that from Boreal North America in a $\sim 2:1$ ratio. Europe strongly dominates the seasonal cycle at Schauinsland, Germany, while many different land regions make small contributions to the cycle at Mauna Loa. Figure 4 also shows a comparison to the observed seasonal cycle from GLOBALVIEW-CO2, with and without an estimated correction for fossil and oceanic influences based on T3L2 model mean archived "pre-subtracted tracer" simulations. This comparison indicates that the CASA model matches the observed cycle reasonably well at these stations, consistent with Gurney et al. (2004).

In contrast, when NEE fluxes from the CLM4 are used as a test case for the PRC, there are clear discrepancies with GLOBALVIEW-CO2 at most stations that transcend ATM uncertainty, even though the range of that uncertainty is large (Fig. 5). At many Northern Hemisphere stations, the CLM4 seasonal cycle is too small in amplitude by about a factor of two, and, at a number of sites, reaches its minimum 1–2 months too early in the summer.

4 Discussion

The validation exercises shown in Figs. 2–3, which compare the results of the pulse-response code driven by CASA NEE fluxes to archived forward simulations with the same fluxes, show that the PRC provides a reasonably faithful representation of the true FS results, especially in the Northern Hemisphere. The main advantages of the PRC are that it runs in seconds and provides an estimate of the spread of results across 13 ATMs. In contrast, a forward simulation with, e.g. a thirteen-year time series of NEE fluxes could take days to weeks, depending on the computer platform, and then

GMDD
5, 2789–2809, 2012

would only provide results from a single ATM. Thus, the PRC involves a relatively small sacrifice in accuracy in exchange for a large improvement in speed, convenience and information about ATM uncertainty.

Since the same NEE fluxes were used for both the PRC and FS calculations, the differences shown in Figs. 2 and 3 reflect the impact of using approximate annual NPP spatial patterns for each month in the PRC, instead of the proper average NEE pattern across that month used in the forward runs. In addition, since the forward simulations were only run out for 2 yr after the 1-yr pulse was turned off, the later FS months were only run out for closer to 24 than 36 months, introducing a time difference in the PRC vs. FS comparison. The difference between the two curves in Fig. 2 should primarily reflect a combination of these 2 factors, assuming that the ATMs behave linearly and that regional results can be added accurately.

As discussed above, an important uncertainty in the PRC predictions is the influence of the spatio-temporal distribution of the unit flux pulse within each land region on the archived T3L2 pulse-response functions. The validation exercises presented above reflect a nearly optimal case with respect to this uncertainty, since the unit pulses in T3L2 were patterned after annual mean CASA NPP, which has a similar distribution to the CASA NEE fluxes used in the validation. As a test of the uncertainty introduced when the spatial pattern of the land fluxes to be evaluated diverges strongly from the CASA NPP distributions, we forced the PRC with the 1990 fossil fuel fluxes used in T3L2 (Andres et al., 1996). This is an extreme test in that fossil fluxes have very dissimilar spatial patterns to NPP. It also has the advantage that the results can be validated against archived T3L2 forward simulations using these same fossil fluxes.

The fossil fuel results are surprisingly good, with PRC v. FS correlations coefficients of $R = 0.80$ or better, and amplitude ratios falling around 1 ± 0.5. Predictably, the PRC performs best at island and remote coastal sites, where local land distributions matter least, and is weakest at sites in continental interiors, where local patterns have greater influence. This extreme test with fossil fuel inputs shows that the PRC results are indeed sensitive to the spatial pattern of the fluxes, and that continental interior sites will

GMDD
5, 2789–2809, 2012

be the least faithfully represented by the PRC when forced with NEE fluxes that depart sharply from the CASA NPP spatial patterns.

The CLM4 results (Fig. 5) are presented primarily as a test case to illustrate the benefit the PRC can provide to land modelers. A detailed assessment of the processes in the CLM4 that lead to discrepancies with observations is beyond the scope of this paper. An earlier application of the PRC code found similar large discrepancies for two other terrestrial ecosystem model NEE fluxes (one of which was an earlier version of the CLM4) (Randerson et al., 2009), suggesting that other process-based terrestrial ecosystem models also may have trouble reproducing the atmospheric CO_2 seasonal cycle. In contrast, the CASA NPP fluxes are not process-based but rather are scaled to agree with empirical satellite data, perhaps explaining why CASA NEE reproduces the observed CO_2 cycle relatively well (Randerson et al., 1997; Gurney et al., 2004).

While earlier terrestrial models focused on NPP, today's more sophisticated mechanistic models simulate the more fundamental processes of gross primary production (GPP). NEE is then the small residual of the two large and opposing fluxes of GPP and total ecosystem respiration. Since process-based models are focused on resolving the physiological processes contributing to the gross fluxes, it is perhaps not surprising that the models have difficulty simulating the NEE balance well enough to accurately reproduce the atmospheric CO_2 cycle.

We have compared PRC results mainly to observations in the Northern Hemisphere rather than the Southern Hemisphere for two principal reasons. First, in the validation exercises above, the PRC performance was weaker at southern sites. This may be due in part to the pulses only being carried out for 36 months in the PRC and for 25 to 36 months in the T3L2 forward simulations. Since Southern Hemisphere sites are far removed from major land regions, the importance of atmospheric mixing and dilution is particularly important at these sites. For some models, even a 36-month simulation may not be adequate to fully capture the smoothing of the atmospheric CO_2 gradient between hemispheres. Notably, full forward simulations with combinations of CASA NEE, ocean and fossil fuel fluxes have also resulted in generally poorer agreement with

GMDD
5, 2789–2809, 2012

observations in the Southern Hemisphere (Randerson et al., 1997; Dargaville et al., 2002; Nevison et al., 2008), which may indicate additional problems with interhemispheric mixing in ATMs.

A second complication in comparing PRC results to observations at southern sites is that oceanic and fossil fuel influences contribute substantially to the (relatively small) CO_2 seasonal cycles in the Southern Hemisphere, making it inappropriate to compare observed CO_2 to modeled atmospheric cycles driven only by NEE influences (Randerson et al., 1997; Nevison et al., 2008). Although one can estimate and add in these contributions as we have done, the comparison of (NEE-driven) modeled and observed CO_2 is heavily influenced by uncertainties in the oceanic and fossil signals (Fig. 5c). In the Northern Hemisphere, the CO_2 seasonal cycle is dominated by NEE, although even there the neglect of fossil fuel and oceanic influences introduces small errors. Forward ATM simulations suggest that the oceanic component of the atmospheric CO_2 accounts typically for $\sim 10 \pm 10\,\%$ the magnitude of the observed cycle and tends to be out of phase with observations (Randerson et al., 1997; Nevison et al., 2008). Fossil fuel generally makes an even smaller contribution than the ocean to the overall seasonal amplitude in atmospheric CO_2, but its importance could be underestimated (although probably only slightly) due to the lack of seasonality in prescribed fossil fluxes (Blasing et al., 2005; Nevison et al., 2008).

Based on the above discussion, we recommend to either (1) directly compare the NEE-driven cycles estimated with the PRC to observed atmospheric CO_2 seasonal cycle in the Northern Hemisphere, ignoring the fossil and oceanic contributions, or (2) estimate the fossil and oceanic influences and subtract them from observed CO_2 before comparing to the NEE-driven PRC results. Approach 2 in principle allows the PRC to be used in either hemisphere, although the relatively large uncertainty associated with fossil and oceanic influences in the Southern Hemisphere undermines the usefulness of the exercise there as a test of model NEE fluxes.

GMDD
5, 2789–2809, 2012

Acknowledgement. We are grateful to the Transcom 3 Level 2 modelers, whose archived results made this paper possible. We also thank Jim Randerson for his help and encouragement in developing the code and Sam Levis for his assistance with CLM4 output.

References

Andres, R. J., Marland, G., Fung, I., and Matthews, E.: A 1° × 1° distribution of carbon dioxide emissions from fossil fuel consumption and cement manufacture, 1950–1990, Global Biogeochem. Cycles, 10, 419–429, 1996.

Baker, D. F.: An inversion method for determining time-dependent surface CO_2 fluxes, in: Inverse Methods in Global Biogeochemical Cycles, Geophys. Monogr., vol. 114, edited by: Kasibhatla, P., et al., AGU, Washington, D.C., 279–293, 1999.

Baker, D. F.: Sources and sinks of atmospheric CO_2 estimated from batch least squares inversions of CO_2 concentration measurements, Ph.D. dissertation, Program in Atmos. and Oceanic Sci., Princeton Univ., Princeton, NJ, 414 pp., 2001.

Baker, D. F., Law, R. M., Gurney, K. R., Rayner, P., Peylin, P., Denning, A. S., Bousquet, P., Bruhwiler, L., Chen, Y.-H., Ciais, P., Fung, I. Y., Heimann, M., John, J., Maki, T., Maksyutov, S., Masarie, K., Prather, M., Pak, B., Taguchi, S., and Zhu, Z.: TransCom 3 inversion intercomparison: impact of transport model errors on the interannual variability of regional CO_2 fluxes, 1988–2003, Global Biogeochem. Cy., 20, GB1002, doi:10.1029/2004GB002439, 2006.

Blasing, T. J., Broniak, C. T., and Marland, G.: The annual cycle of fossil-fuel carbon dioxide emissions in the United States, Tellus, 57B, 107–115, 2005.

Bonan, G. B. and Levis, S.: Quantifying carbon-nitrogen feedbacks in the Community Land Model (CLM4), Geophys. Res. Lett., 37, L07401, doi:10.1029/2010GL042430, 2010.

Dargaville, R. J., Heimann, M., McGuire, A. D., Prentice, I. C., Kicklighter, D. W., Joos, F., Clein, J. S., Esser, G., Foley, J., Kaplan, J., Meier, R. A., Melillo, J. M., Moore III, B., Ramankutty, N., Reichenau, T., Schloss, A., Sitch, S., Tian, H., Williams, L. J., and Wittenberg, U.: Evaluation of terrestrial carbon cycle model through simulations of the seasonal cycle of CO_2: results from transient simulations consisting of increasing CO_2, climate and land-use effects, Global Biogeochem. Cy., 16, 1092, doi:10.1029/2001GB001426, 2002.

GMDD

5, 2789–2809, 2012

Forster, P., Ramaswamy, V., Artaxo, P., Berntsen, T., Betts, R., Fahey, D. W., Haywood, J., Lean, J., Lowe, D. C., Myhre, G., Nganga, J., Prinn, R., Raga, G., Schulz, M., and Van Dorland, R.: Changes in atmospheric constituents and in radiative forcing, in: Climate Change 2007: The Physical Science Basis. Contribution of Working Group I to the Fourth Assessment Report of the Intergovernmental Panel on Climate Change, Cambridge University Press Cambridge, UK and New York, NY, USA, 2007.

Friedlingstein, P., Cox, P., Betts, R., Bopp, L., von Bloh, W., Brovkin, V., Cadule, P., Doney, S., Eby, M., Fung, I., Bala, G., John, J., Jones, C., Joos, F., Kato, T., Kawamiya, M., Knorr, W., Lindsay, K., Matthews, H. D., Raddatz, T., Rayner, P., Reick, C., Roeckner, E., Schnitzler, K.-G., Schnur, R., Strassmann, K., Weaver, A. J., Yoshikawa, C., and Zeng, N.: Climate-carbon cycle feedback analysis: results from the C4MIP model intercomparison, J. Climate, 19, 3337–3353, 2006.

Fung, I. Y., Tucker, C. J., and Prentice, K. C.: Application of advanced very high resolution reiometer vegetation index to study atmosphere-biosphere exchange of CO_2, J. Geophys. Res., 92, 2999–3015, 1987.

GLOBALVIEW-CO2: Cooperative Atmospheric Data Integration Project – Carbon Dioxide, CD-ROM, NOAA GMD, Boulder, Colorado, available at: ftp://ftp.cmdl.noaa.gov, Path: ccg/co2/GLOBALVIEW, 2010.

Gurney, K. R., Law, R. M., Denning, A. S., Rayner, P. J., Pak, B. C., Baker, D., Bousquet, P., Bruhwile, R., Chen, Y.-H., Ciais, P., Fung, I. Y., Heimann, M., John, J., Maki, T., Maksyutov, S., Peylin, P., Prather, M., and Taguchi, S.: Transcom 3 inversion intercomparison: model mean results for the estimation of seasonal carbon sources and sinks, Global Biogeochem. Cy., 18, GB1010, doi:10.1029/2003GB002111, 2004.

Keeling, C. D., Chin, J. F. S., and Whorf, T. P.: Increased activity of northern vegetation inferred from atmospheric CO_2 measurements, Nature, 382, 146–149, 1996.

Nevison, C. D., Mahowald, N., Doney, S., Lima, I., van der Werf, G., Randerson, J., Baker, D., Kasibhatla, P., and McKinley, G.: Contribution of ocean, fossil fuel, land biosphere and biomass burning carbon fluxes to seasonal and interannual variability in atmospheric CO_2, J. Geophys. Res., 113, G01010, doi:10.1029/2007JG000408, 2008.

Randerson, J. T., Thompson, M. V., Conway, T. J., Fung, I. Y., and Field, C. B.: The contribution of terrestrial sources and sinks to trends in the seasonal cycle of atmospheric carbon dioxide, Global Biogeochem. Cy., 11, 535–560, 1997.

GMDD
5, 2789–2809, 2012

Randerson, J. T., Hoffmann, F. M., Thornton, P. E., Mahowald, N. M., Lindsay, K., Lee, Y. H., Nevison, C. D., Doney, S. C., Bonan, G., Stoeckli, R., Covey, C., Running, S. W., and Fung, I. Y.: Systematic assessment of terrestrial biogeochemistry in coupled climate-carbon models, Glob. Change Biol., 15, 2462–2484, doi:10.1111/j.1365-2486.2009.01912.x, 2009.

Rotty, R. M.: Estimates of seasonal variation in fossil-fuel CO_2 emissions, Tellus B, 39, 184–202, 1987.

Takahashi, T., Wanninkhof, R. H., Feely, R. A., Weiss, R. F., Chipman, D. W., Bates, N., Olafsson, J., Sabine, C., and Sutherland, S. C.: Net sea-air CO_2 flux over the global oceans: An improved estimate based on the sea- air pCO_2 difference, in: Proceedings of the 2nd International Symposium: CO_2 in the Oceans, the 12th Global Environmental Tsukuba, 18–22 January 1999, Tsukuba Center of Institutes, edited by: Nojiri, Y., Natl. Inst. for Environ. Stud., Environ. Agency of Jpn., Tokyo, 1999.

Takahashi, T., Sutherland, S. C., Sweeney, C., Poisson, A., Metzl, N., Tillbrook, B., Bates, N., Wanninkhof, R., Feely, R. A., Sabine, C., Olafsson, J., and Nojiri, Y: Global sea-air flux based on climatological surface ocean pCO_2, and seasonal biological and temperature effects, Deep-Sea Res. Pt. II, 49, 1601–1622, 2002.

Taylor, K. E.: Summarizing multiple aspects of model performance in a single diagram, J. Geophys. Res., 106, 7183–7192, 2001.

GMDD

5, 2789–2809, 2012

Table 1. Expanded view of the structure of **H** (for a given ATM, region and sampling site) spanning 48 "measurement" months and 12 "emission" months (red rectangle in Fig. 1). The pulse-response functions comprise a repeating 47-month band of measurement years, because the January pulse is released in month 1 of year 1 and allowed to decay through month 12 of year 3, while the December pulse is released in month 12 of year 1 and allowed to decay through month 11 of year 4, etc.

Mon	1	2	...	12
1	$h_{1,1}$	0	...	0
2	$h_{2,1}$	$h_{2,2}$	...	0
...	...	...	...	...
11	$h_{11,1}$	$h_{11,2}$	...	0
12	$h_{12,1}$	$h_{12,2}$	...	$h_{12,12}$
...	...	...	...	...
36	$h_{36,1}$	$h_{36,2}$	...	$h_{36,12}$
37	h_{∞}	$h_{37,2}$	...	$h_{37,12}$
38	h_{∞}	h_{∞}	...	$h_{38,12}$
...	...	...	...	...
47	h_{∞}	h_{∞}	h_{∞}	$h_{47,12}$
48	h_{∞}	h_{∞}	h_{∞}	h_{∞}

GMDD
5, 2789–2809, 2012

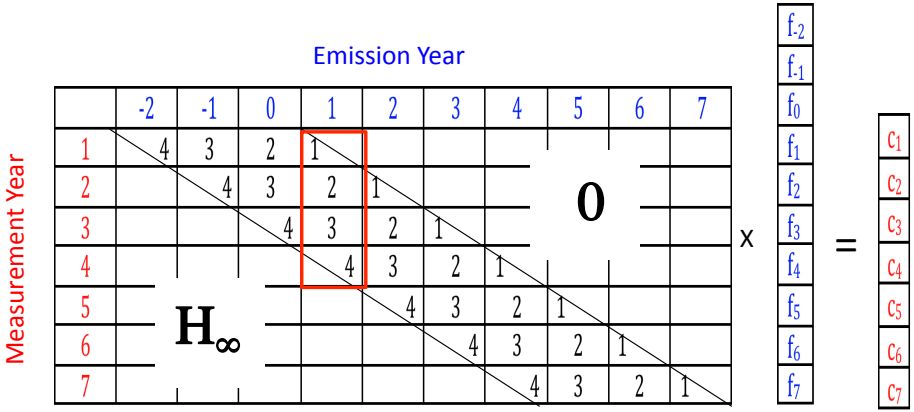

Fig. 1. Structure of **H** and the corresponding matrix multiplication $\mathbf{H}f = c$. $\mathbf{H}_\infty$ is the atmospheric signature of an infinitely well-mixed 1 Pg C pulse of atmospheric CO_2. In this example, the input fluxes f span 10 emission years, 3 of which precede but still influence the first measurement year, but could extend over any number of years if **H** were expanded accordingly.

GMDD
5, 2789–2809, 2012

Estimating CO_2 seasonal cycles from NEE

C. D. Nevison et al.

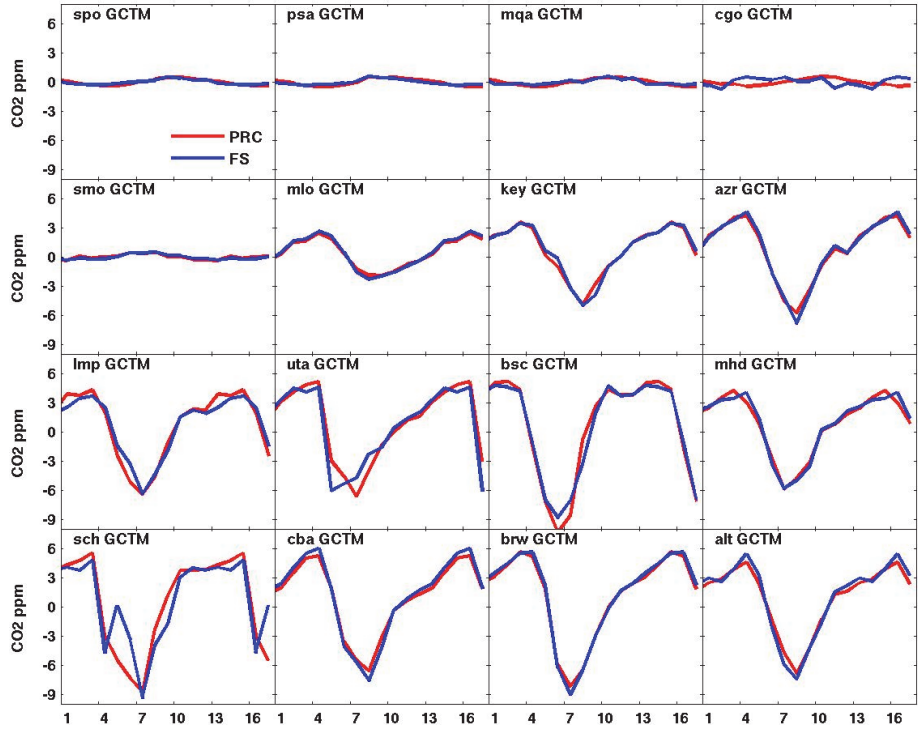

Fig. 2. Mean seasonal cycle in atmospheric CO_2 produced by forcing the GCTM atmospheric transport model with monthly mean NEE fluxes from the CASA terrestrial ecosystem model. Archived results from T3L2 GCTM forward simulations (blue) are compared to estimates using the GCTM variant of the pulse-response code (red) at 16 stations: spo (South Pole), psa (Palmer Station), mqa (Macquarie), cgo (Cape Grim), smo (Samoa), mlo (Mauna Loa), key (Key Biscayne, Florida), azr (Azores), lmp (Lampudesa, Italy), uta (Utah), bsc (Black Sea, Romania), mhd (Mace Head, Ireland), sch (Shauinsland, Germany), cba (Cold Bay, Alaska), brw (Barrow, Alaska), alt (Alert, Greenland).

GMDD
5, 2789–2809, 2012

Estimating CO_2 seasonal cycles from NEE

C. D. Nevison et al.

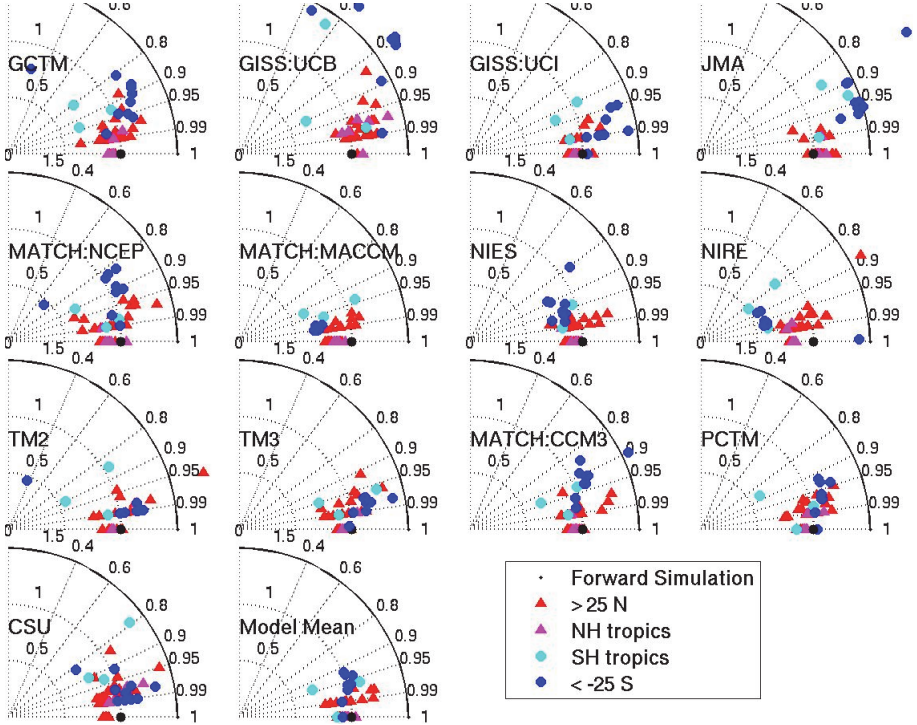

Fig. 3. Taylor diagrams illustrating the agreement in phase and amplitude between the pulse-response code and the archived T3L2 forward simulations forced by monthly mean NEE fluxes from the CASA terrestrial ecosystem model. The reference point at a radius of 1 and correlation coefficient of 1.0 represents perfect agreement with the forward simulation. Each circle on the Taylor diagram represents one of 60 sampling sites, color coded by latitude.

GMDD
5, 2789–2809, 2012

Estimating CO_2 seasonal cycles from NEE

C. D. Nevison et al.

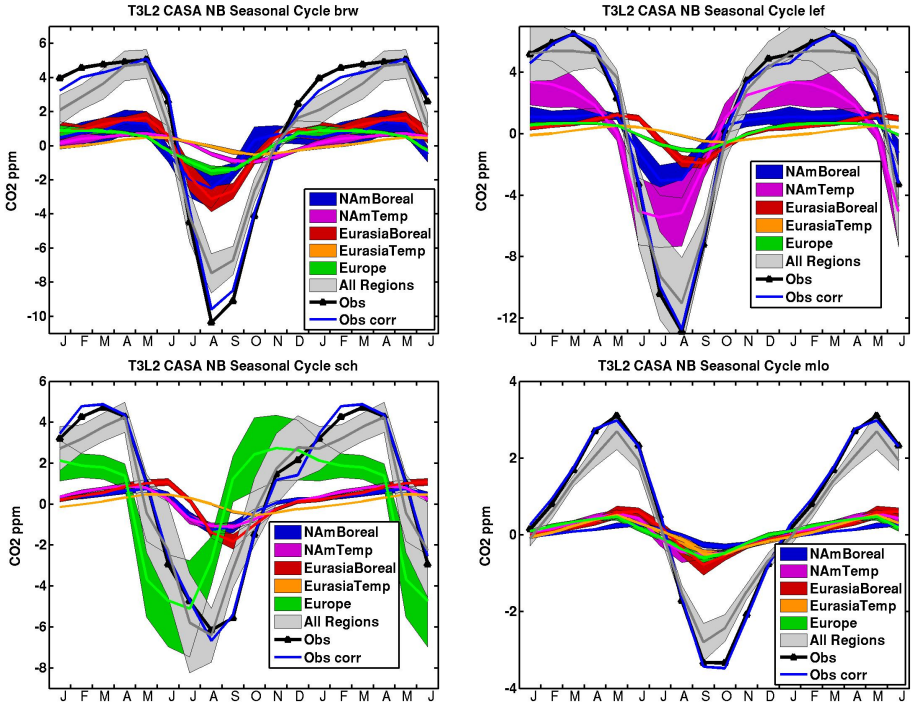

Fig. 4. Regional contribution to the mean seasonal cycle in atmospheric CO_2, as predicted by the pulse-response code forced with CASA neutral biosphere NEE fluxes. Envelopes show the mean ± the standard deviation of the 13 T3L2 models. For clarity, only the five northern temperate and boreal regions, which dominate the cycles, are shown: **(a)** Barrow, Alaska, **(b)** Park Falls, Wisconsin, **(c)** Schauinsland, Germany, **(d)** Mauna Loa. The observed mean seasonal cycle is shown in black (uncorrected) and blue (corrected for model mean fossil fuel and ocean signals from archived T3L2 forward simulations).

GMDD
5, 2789–2809, 2012

Estimating CO_2 seasonal cycles from NEE

C. D. Nevison et al.

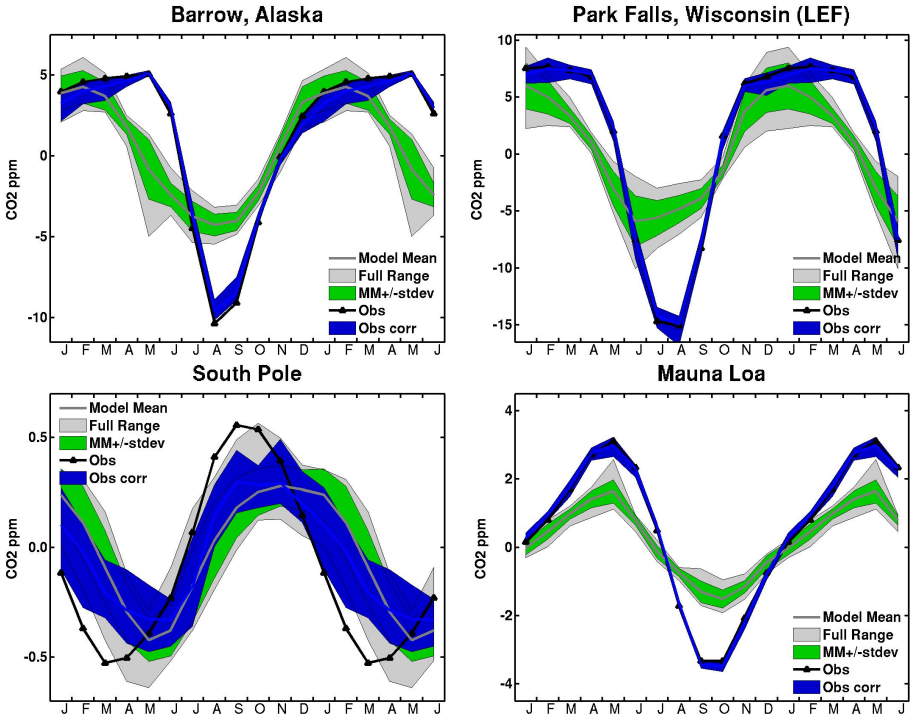

Fig. 5. Mean seasonal cycle in atmospheric CO_2, as predicted by the pulse-response code forced with 1993–2005 NEE fluxes from the Community Land Model (CLM4.0). Green envelopes show the mean ± the standard deviation of the 13 T3L2 models. Grey envelopes show the full range of variability among the 13 T3L2 models: **(a)** Barrow, Alaska, **(b)** Park Falls, Wisconsin, **(c)** South Pole, **(d)** Mauna Loa. Observations are shown in black (uncorrected) and blue (corrected for fossil and ocean signals from archived T3L2 forward simulations). The blue envelopes show the full range of ATM uncertainty associated with the fossil and ocean corrections.

GMDD
5, 2789–2809, 2012

Estimating CO_2 seasonal cycles from NEE

C. D. Nevison et al.

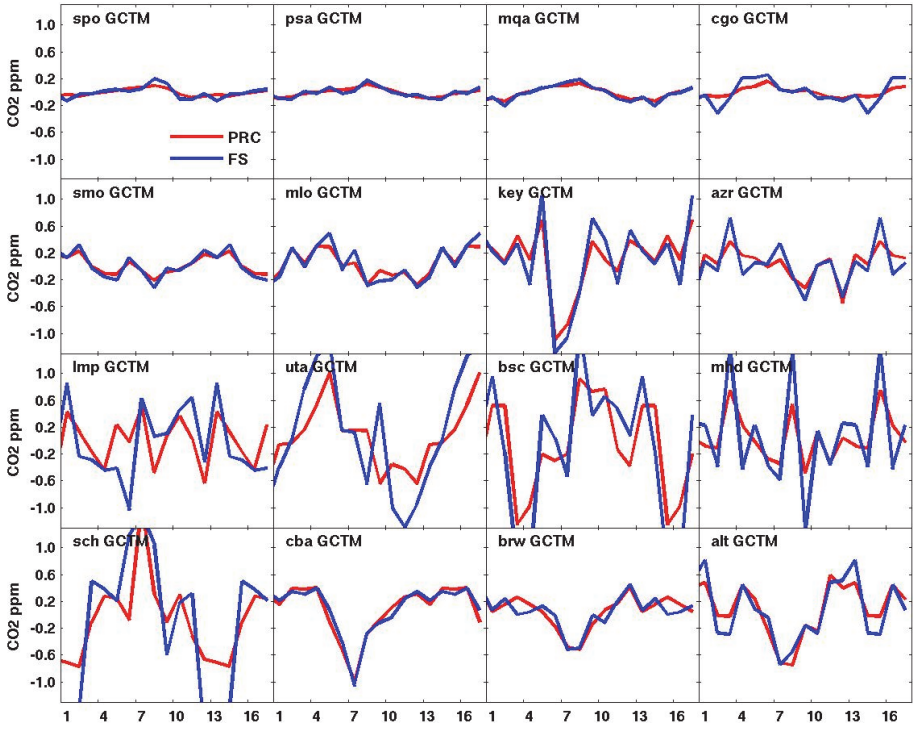

Fig. 6. Mean seasonal cycle in atmospheric CO_2 produced by forcing the GCTM atmospheric transport model with 1990 fossil fuel and cement carbon emissions (Andres et al., 1996). Archived results with these same emissions from T3L2 GCTM forward simulations (blue) are compared to estimates using the GCTM variant of the pulse-response code (red) at 16 stations (see Fig. 2 for list).

GMDD
5, 2789–2809, 2012

Estimating CO_2 seasonal cycles from NEE

C. D. Nevison et al.

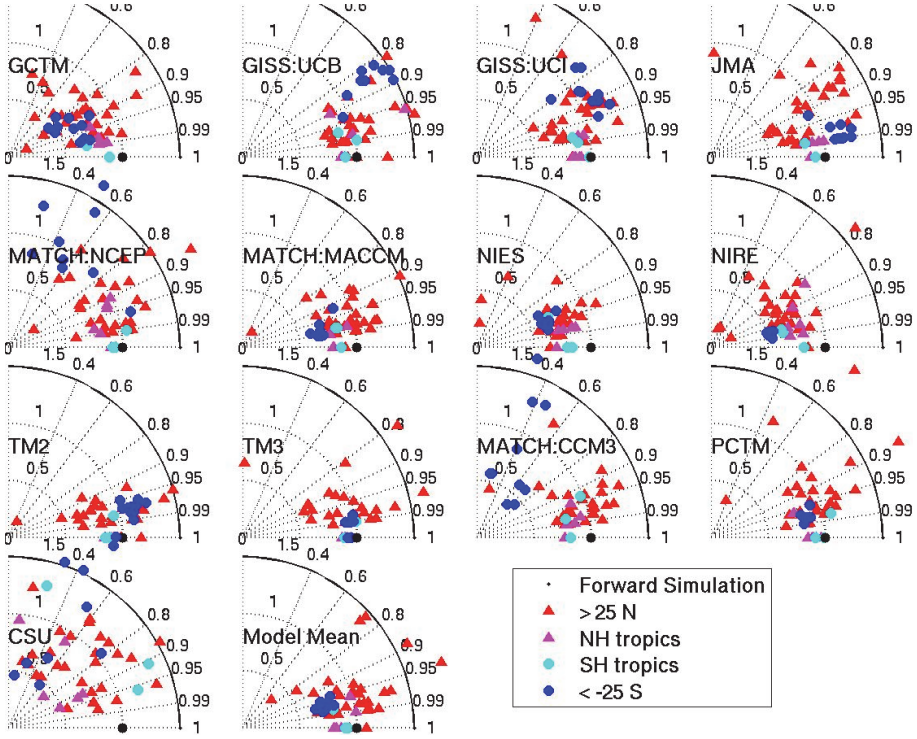

Fig. 7. Taylor diagrams illustrating the agreement in phase and amplitude between the pulse-response code and the archived T3L2 forward simulations forced by 1990 fossil fuel and cement carbon fluxes (see Fig. 3 for details of Taylor diagrams).

GMDD
5, 2789–2809, 2012